

Synthesis and characterization of amphiphilic triblock copolymers by iron mediated atom transfer radical polymerization

Khalid Ibrahim, Paul Starck, Barbro Löfgren, and Jukka Seppälä *

Helsinki University of Technology, Department of Chemical Technology, Laboratory of Polymer Technology, P.O. Box 6100, FI-02015 TKK, Finland.

Abstract: Atom transfer radical polymerization (ATRP) of methyl methacrylate (MMA) and *n*-Butyl methacrylate (*n*-BMA) was initiated by a poly(oxyethylene) chloro telechelic macroinitiator synthesized by esterification of poly(ethylene glycol) PEG with 2-chloro propionyl chloride. The polymerization carried out in bulk at 90 °C catalyzed by bis-triphenylphosphine iron(II) chloride tetrahydrate ($\text{FeCl}_2 \cdot 4\text{H}_2\text{O}(\text{PPh}_3)_2$) has been found to lead to A-B-A amphiphilic triblock copolymers with MMA or *n*-BMA as the A block and PEO as the B block. The kinetic study showed that the polymerization is first order with respect to monomer concentration. Moreover, the experimental molecular weights of the block copolymers increased linearly with monomer conversion and the molecular weight distribution was acceptable narrow at the end of the reaction. These block copolymers turned out to be water-soluble through adjusting the content of the PEO blocks. In the case of water insoluble block copolymers only one glass transition temperature was detected when the PEO content was small (monomer/macroinitiator molar ratio (M/I) = 300). Upon increasing the amount of PEO (M/I = 100 and 50) in the copolymer, two glass transitions were detected, indicating phase separation as in the case of water-soluble ones. The macroinitiator and the corresponding triblock copolymers were characterized by FT-IR, ^1H NMR, GPC analysis, DMA and DSC.

Keywords: Block copolymers, Atom transfer radical polymerization, Methyl methacrylate, Poly (oxyethylene) chloro telechelic macroinitiator, Glass transition temperature.

Introduction

Atom transfer radical polymerization (ATRP) has provided a powerful tool for macromolecular design since it was first reported by Matyjaszewski and others.¹⁻⁵ This technique offers a convenient method for the preparation of A-B and A-B-A block copolymers by using either sequential monomer addition or macroinitiator.^{6,7,8} The increasing interest of hydrophilic-hydrophobic block copolymers is due to the improvement of the synthesis techniques and to their application possibilities as biomaterials, drug carriers, stabilizers in suspensions or emulsions, surface modifying agents, adhesives and coatings, etc.⁹ Most of the amphiphilic block copolymers of this type comprise poly(ethylene glycol) (PEG) as hydrophilic blocks, whereas the hydrophobic blocks are poly(methyl methacrylate), polystyrene, etc.^{7,8,10,11} PEG, in addition to its adjustable water solubility, has the advantage to be biocompatible.

Since we have earlier studied iron-based catalysts for meth(acrylates),¹²⁻¹⁴ we will now in this article report the synthesis of A-B-A triblock copolymers (PMMA-b-PEO-b-PMMA) and (PBMA-b-PEO-b-PBMA), as outlined in Scheme 1, using bis-triphenylphosphine iron (II) chloride tetrahydrate ($\text{FeCl}_2 \cdot 4\text{H}_2\text{O}(\text{PPh}_3)_2$) as catalyst in bulk at 90 °C. The same conditions were used to produce water-soluble (PMMA-b-

PEO-b-PMMA) triblock copolymers. The water solubility was controlled by adjusting the mass percent of the PEO blocks of different molecular weights.

Experimental

Materials

Methyl methacrylate (MMA) (Aldrich, 99%) was purified by passing it through a column of activated basic alumina to remove inhibitor. It was then stored under nitrogen at $-15\text{ }^{\circ}\text{C}$. *n*-Butyl methacrylate (*n*-BMA) (*purum* grade from Fluka) was purified by washing with 5% sodium hydroxide aqueous solution, followed by washing with water. The organic portion was dried for 24 h under anhydrous sodium sulfate, filtered, and finally distilled under reduced pressure. It was stored under nitrogen at $-15\text{ }^{\circ}\text{C}$. Triphenylphosphine 99% (Merck) and $\text{FeCl}_2\cdot 4\text{H}_2\text{O}$ 99% (Aldrich) were used without purification. PEG (2000, 6000, 10,000, 20,000 g/mol) (Aldrich) was dried in vacuum for 24 h before use. 4-Dimethyl amino pyridine (DMAP) 99% (Fluka) was recrystallized from toluene. Triethyl amine (TEA) 99% (Acros) was refluxed with *p*-toluene sulfonyl chloride distilled and stored over CaH_2 . 2-Chloro propionyl chloride 97% (Fluka) was used without further purification. All other reagents were used as received.

Synthesis of catalysts

$\text{FeCl}_2\cdot 4\text{H}_2\text{O}(\text{PPh}_3)_2$ was synthesized according to the method described in details in our earlier paper.¹⁴

Polymerization

Polymerization of block copolymers was carried out under dry nitrogen in a dried Schlenk tube equipped with a magnetic stirring bar. The tube was charged with the required amount of macroinitiator and catalyst, sealed with a rubber septum, and then degassed to remove oxygen. Degassed methacrylate monomer was added using a nitrogen-purged syringe, and the tube was degassed and back-filled with nitrogen three times. The content was stirred for 5 minutes. Finally, the tube was immersed in an oil bath preheated to 90 °C. After a given time, the reaction was stopped, and the reaction mixture was cooled to room temperature and the crude products were dissolved in dichloromethane. The obtained polymer solution was passed over alumina to remove the catalyst, and the polymer was precipitated with an excess amount of hexane. The precipitated polymer was extracted twice with distilled water at room temperature to remove possible unreacted PEO macroinitiator and then immersed in cold diethyl ether, and dried in vacuum at room temperature.

Characterization

The dried product was characterized by FT-IR, ¹H-NMR, DSC, DMA and GPC techniques and the conversion was determined by gravimetry.

FT-IR spectra of the macroinitiator and block copolymers were recorded on a Nicolet Magna FT-IR spectrometer using the KBr pellet technique. The molecular weights were determined by room temperature SEC (Waters System Interface model, Waters 510 HPLC Pumps, Waters Differential Refractometer, Waters 700 satellite Wisp, and four linear PL gel columns: 10⁴, 10⁵, 10³ and 10² Å connected in series). Chloroform was used as solvent and eluent. The samples were filtered through a 0.5 µm Millex

SR filter. Injected volume was 200 μl and the flow rate was 1 ml min^{-1} . Nearly monodisperse polystyrene standards in the range 2×10^6 -150 g/mol were used for primary calibration.

The ^1H NMR spectra of the polymer were recorded using a Varian Inc. (Palo Alto, CA) Gemini 2000XL NMR spectrometer operated at 300 MHz. The polymer solution was prepared by dissolving about 50 mg of polymer in 3 ml of deuterated chloroform (CDCl_3).

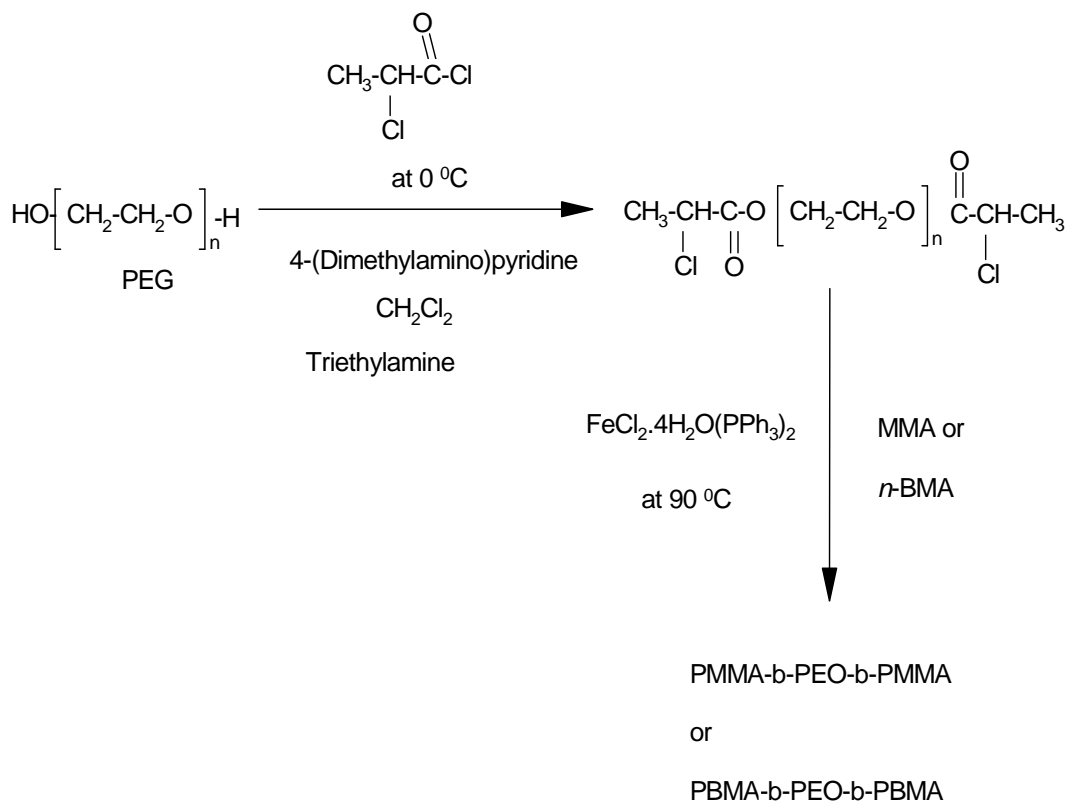
Differential scanning calorimetry (DSC) runs were performed on a Perkin-Elmer DSC 7 apparatus equipped with a liquid nitrogen cooling system. Calibration was made with Indium under a nitrogen atmosphere. Samples (18-20 mg) sealed in aluminium pans were quenched from room temperature to $-60\text{ }^\circ\text{C}$ and then scanned at $15\text{ }^\circ\text{C/min}$ to $+140\text{ }^\circ\text{C}$, kept at this temperature for 5min and then cooled back to $-60\text{ }^\circ\text{C}$ at $15\text{ }^\circ\text{C/min}$. After 5 min at this temperature a final heating run was made at $15\text{ }^\circ\text{C/min}$ to $140\text{ }^\circ\text{C/min}$. Melting (T_m) and crystallization (T_c) temperatures were taken from the peak maxima in the second melting scan and the cooling scan, respectively. The value for the glass transition (T_g) are reported as the temperature by which one-half of the specific heat (ΔC_p) increase in glass transition region has occurred.

Dynamic mechanical analysis (DMA) technique (Perkin-Elmer DMA 7 in tensile mode) was used for some samples to confirm the presence or absence of phase separation. Tensile films were prepared by solvent casting and temperature sweeps were conducted from $-80\text{ }^\circ\text{C}$ at a heating rate of $4\text{ }^\circ\text{C/min}$.

Results and Discussion

1. Synthesis of PMMA-b-PEO-b-PMMA triblock copolymers

In the synthesis of PMMA-b-PEO-b-PMMA triblock copolymers the telechelic macroinitiator was prepared by an esterification reaction between PEG and 2-chloro propionyl chloride⁷ (Scheme 1). By GPC analysis it was found that poly(oxyethylene) chloro telechelic macroinitiator (Cl-PEO-Cl) did not show any reduction in molecular weight, since narrow symmetrical peaks were observed at essentially the same position as for the starting PEG. The data are given in Table 1. As expected, M_n (GPC) data are less accurate than M_n (NMR) as GPC calibration was carried out with polystyrene standards.



Scheme 1. Preparation of PEO macroinitiator and the corresponding triblock copolymer.

Table 1 here

The commercially available triphenyl phosphine is an efficient ligand for the iron mediated ATRP of meth(acrylate) polymers.^{12,13,15,16} Triblock A-B-A copolymers were synthesized using the poly(oxyethylene) chloro telechelic macroinitiator where A = MMA and B = PEO, the polymerization of MMA was conducted with $(\text{FeCl}_2 \cdot 4\text{H}_2\text{O}(\text{PPh}_3)_2)$ in bulk at 90 °C. Figure 1 presents a kinetic plot of conversion versus time, showing that monomer conversion increases with time, and that the reaction rate is relatively fast (conversion >60% in 90 minutes) indicating an efficient catalyst system.

Figure 1 here

Figure 2 here

The linear semilogarithm plot of $\ln([\text{M}]_0 / [\text{M}]_t)$ vs time (where M_0 is the initial concentration of the monomer, and M_t is the monomer concentration at any time), illustrated in Figure 2, indicates that the concentration of growing radicals is constant. Moreover Figure 2 shows an insignificant induction period, which is not observed when low molecular weight initiators are used.¹⁷ The slow initiation is in agreement with results reported by Bednarek et al.¹¹ for ATRP of MMA with poly(oxyethylene) macroinitiator.

Figure 3 here

Figure 3 reveals that the molecular weight of the product gradually increases with monomer conversion. The molecular weights increase from a starting value, which correspond to the initial molecular weight of Cl-PEO-Cl macroinitiator. The final properties of the product are summarized in Table 2. It is noted that M_n (NMR) is

much closer to M_n , than M_n (GPC) (in the present case for sample no.4 M_n (NMR) = 19,000 g/mol). This phenomenon can be ascribed to the slow initiation of the macroinitiator and to the difference in hydrodynamic volumes compared with polystyrene standards. In such cases, the ^1H NMR is more reliable approach to determining the molecular weight.¹⁸

Table 2 here

Figure 4 here

GPC curves of the Cl-PEO-Cl macroinitiator and the resulting triblock copolymers obtained in bulk are presented in Figure 4. The GPC curves indicate that PMMA-b-PEO-b-PMMA block copolymers are formed, since the entire elution curves are shifted linearly towards higher molecular weights. Also the triblock obtained has acceptable narrow molecular weight distribution (M_w/M_n) value below 1.5.

Representative FT-IR spectra of PEG 2000, Cl-PEO-Cl macroinitiator, and PMMA-b-PEO-b-PMMA block copolymers are shown in Figure 5. In the spectra of PEG, the peaks for -C-O-C- and -OH stretching are observed at 1113 cm^{-1} and at $3300\text{-}3600\text{ cm}^{-1}$, respectively. After the esterification reaction, the -OH peaks disappeared and instead the absorption peak of C=O at 1750 cm^{-1} was observed in the spectrum. This suggests that the -OH end groups of the PEG have been converted quantitatively to 2-chloro propionate end groups. It should be noted that from Figure 5 (a) KBr pellet contains some moisture which also appeared in the Cl-PEO-Cl macroinitiator. The spectrum of the triblock copolymer exhibits strong peaks at 1735 cm^{-1} (C=O of the ester group) and 1150 cm^{-1} , characteristic for PMMA segments. An indication of PEG segments are seen from the absorbance peaks at 3500 cm^{-1} (-OH stretching) and 1113

cm^{-1} (assigned to $-\text{C}-\text{O}-\text{C}$ of the PEO chain). PMMA methylene peaks at 2950, 1482 and 1398 cm^{-1} were also observed in the block copolymers.¹⁹

^1H NMR spectra of Cl-PEO-Cl macroinitiator, PMMA and PMMA-b-PEO-b-PMMA are presented in Figure 6. The spectrum of the macroinitiator (Fig. 6a) shows a small signal at 4.30 ppm due to the substituted PEG and a signal at 3.62 ppm due to the $\text{CH}_2-\text{CH}_2-\text{O}$ resonance. In the spectrum of the triblock copolymer (Fig. 6c) the $\text{CH}_2\text{CH}_2-\text{O}$ resonance of PEG at 3.63 ppm and the $\text{O}-\text{CH}_3$ protons of PMMA at 3.58 ppm are both noticed as well as the methylene proton peak at 1.88 ppm and the α -methyl proton peak at 0.83 ppm, already seen in the spectrum of the PMMA (Fig. 6b).

Figure 6 here

The glass transition temperatures (T_g) were measured by DSC to check the phase behaviour of the triblock copolymers. T_g 's of $-39\text{ }^\circ\text{C}$ and $122\text{ }^\circ\text{C}$ were obtained for PEG 2000 and PMMA, respectively. The T_g of our PMMA, prepared by ATRP is very close to the $T_g = 125\text{ }^\circ\text{C}$, reported for this type of PMMA by Moineau et al.²⁰ and Quin et al.²¹, respectively. Only a single glass transition temperature, appearing above $100\text{ }^\circ\text{C}$ but below the T_g of the PMMA, is observed for all block copolymers. This is an indication that these block copolymers represent only one phase. The absence of a T_g of any PEO block was further confirmed by DMA (see next section). It is the low concentration of the macroinitiator which may explain why no transition at the T_g range of the Cl-PEO-Cl macroinitiator is detected.²²

In order to investigate the effect of the macroinitiator concentration on the behaviour of the block copolymers, the monomer to macroinitiator molar ratio was decreased

from 300 to 100 and further to 50, these increasing the amount of PEO blocks in the copolymers. In these cases two glass transitions were detected by DSC, which confirms that phase separation has taken place. The effect of increased chain length was also studied by using a PEG of molecular weight 10000 g/mol instead of 2000 g/mol in the polymerizations. This change gave also two T_g transitions, still confirming the existence of phase separation.

The T_g of the block copolymers decreases as the molecular weight of the poly(methyl methacrylate) block increases (Figure 7 and Table 2), in accordance with earlier reports.²³ As the molecular weight increases, a slight broadening of the transition and a corresponding reduction of ΔC_p is noticed.

Figure. 7 here

2. Synthesis of *n*-BMA-*b*-PEO-*b*-*n*-BMA triblock copolymers

To further study the versatility of iron as a catalyst for A-B-A triblock copolymerization, *n*-BMA was used as the outer block under the same polymerization conditions as for polymerizing MMA. In this case, the reaction medium was less viscous than that for MMA, and no polymer was formed before 90 minutes. After this time the reaction was stopped to get comparable results with PMMA polymerizations. The conversion was only 36%, and the $M_{n,theo}$ was not in good agreement with M_n (GPC), but in good agreement with M_n (NMR): (M_n (GPC) = 170,000 g/mol, where $M_{n,theo}$ = 20,000 g/mol, and M_n (NMR) = 16,000 g/mol), and the molecular weight distributions were acceptable narrow (M_w/M_n = 1.54). One possible

explanation is that concentration of iron (II) halide decreased due to the low solubility of the complex.

Figure 8 exhibits the ^1H NMR spectrum of PBMA homopolymers and PBMA-b-PEO-b-PBMA copolymers. The signal at $\delta = 3.94$ ppm is attributed to the ester methyl proton in the PBMA unit.

Figure 8 here

By DSC, neither melting, crystallization peaks, nor glass transitions of PEO were noticed at all in the block copolymers. The PBMA block showed a T_g at 12°C , which is much lower than the T_g found for PBMA (30.2°C), a value which is very close to the $T_g = 33.1^\circ\text{C}$ of an ATRP mediated PBMA, reported by Martin-Gomis et al.²⁴ Thus it is noticed that the T_g , related to the outer PBMA segments, moves to a lower temperature. In order to confirm the absence of T_g of PEO blocks, some runs of cast films of copolymer samples were performed by dynamic mechanical analysis (DMA) (Figure 9). DMA is known to be much more sensitive in detecting glass transitions than DSC. However, the loss modulus (E'') and the $\tan \delta$ curves of the PBMA-b-PEO-b-PBMA copolymer (Figure 9 a) do not show any peaks below 0°C , which confirms the absence of longer crystalline PEO blocks in the copolymer. The loss modulus exhibits a peak at 22°C , which corresponds to the glass transition of the rigid PBMA block. It is well known that differences exist between the T_g s determined by DSC and DMA, respectively. This explains the deviation from the T_g , 12°C , obtained by DSC. The loss modulus and $\tan \delta$ curves of the PMMA-b-PEO-b-PMMA copolymer (curve b) do not either exhibit any transitions in the subambient region, which confirms the absence of T_g of the PEO segment. The relaxation related to the

glass transition of the PMMA block cannot be exactly measured under tension, since the films obtained by solvent casting are too weak at that temperature. However, according to the Figure 9, the T_g region is started above 100 °C. Using the earlier described polymerization conditions block copolymers are formed, which do not show any phase separation.

Figure 9 here

3. Synthesis of water-soluble block copolymers

From earlier investigations ²⁵ it appears that as soon as the initial weight percentage of the hydrophobic comonomer becomes higher than 10 wt%, the corresponding copolymer is water-insoluble. By ATRP technique, a series of PMMA-b-PEO-b-PMMA triblock copolymers with different molecular weights and compositions were synthesized. Molecular weights of PEG for A1, A2, A3, A4 is 20,000 g/mol; for B 10,000 g/mol; for C1, C2, C3 6000 g/mol, and for D1,D2 2000 g/mol. Table 3 shows the molecular characteristics data of water-soluble/dispersable triblock copolymers of PMMA-b-PEO-b-PMMA. The Table reveals that controlled water-soluble (narrow molecular weight distribution, agreement between experimental and theoretical molecular weights) copolymers have been synthesized by means of the $\text{FeCl}_2 \cdot 4\text{H}_2\text{O}$ $(\text{PPh}_3)_2$ catalytic system.

Table 3 here

The differences in melting and crystallization behaviour, as well as, the glass transitions were measured by DSC, and the obtained data are summarized in Table 4. According to the GPC analyses the molecular weight data of the starting PEG and corresponding macroinitiator were about the same and this explains their similar glass transition temperatures. However, the melting temperatures and the crystallization

temperatures of the macroinitiators were clearly lower than those of the corresponding PEGs, and the synthesized block copolymers displayed still lower crystallization temperatures. The poly(ethylene oxide) segments in the copolymers are shorter than in the macroinitiators and in the starting PEGs. Therefore, these shorter segments will need longer times (lower temperatures) to crystallize. The very slow crystallization of copolymer B may be caused by a fractionated crystallization process, which is leading to PEO confined into cylinders or spheres.²⁶ Figure 10 displays the melting endotherms of two block copolymers, A1 and A4, and the corresponding macroinitiator Cl-PEO(20K)-Cl, used in their synthesis. A slight decrease in the T_m of the PEO component is seen with decreasing weight fraction of PEO. A similar trend can also be noticed for the C series (Table 4). The inset curves, which are magnified in the heat flow scale, demonstrate the presence of two glass transitions, which suggests that the block copolymers are phase separated. The high amount of PEO segments in the triblock copolymer explains why no clear shift in their T_g -values is observed, but the T_g s of the PMMA segments are shifted by 20 °C to lower temperatures, compared to the T_g of pure PMMA. However, the amount of PMMA blocks in the triblock copolymer had no influence on the T_g -values of the PMMA block.

Table 4 here

Fig.10 here

Conclusion

At high monomer to macroinitiator molar ratios, polymerization of MMA and n-BMA initiated with poly (oxyethylene) chloro telechelic macroinitiator and catalyzed by $(\text{FeCl}_2 \cdot 4\text{H}_2\text{O}(\text{PPh}_3)_2)$ proceeds in a controlled manner in accordance to the ATRP mechanism, leading to A-B-A triblock copolymers. No melting and crystallization peaks, or glass transitions of PEO are noticed at all in these kinds of block copolymers and the T_g related to the outer segments moves to a lower temperature. However, at low monomer to macroinitiator molar ratios, glass transitions of the both PEO and PMMA blocks were detected by DSC. This confirms that phase separation has taken place. The use of poly(ethylene oxides) of higher chain length in the polymerizations also lead to phase separation of the blocks. The presence of two separate glass transitions is furthermore seen in water-soluble triblock copolymers.

According to our experiments, triphenyl phosphine is proven to be a versatile ligand in iron mediated ATRP, when A-B-A triblock copolymers using poly (oxyethylene) chloro telechelic macroinitiator are synthesized.

The authors are thankful to National Technology Agency (TEKES) for their financial support.

References

1. Wang, JS.; Matyjaszewski K. *J Am Chem Soc* 1995, 117, 5614.
2. Matyjaszewski, K.; Xia, J. *Chem. Rev.* 2001, 101, 2921.
3. Kato, M.; Kamigaito, M.; Sawamoto, M.; Higashimura, T. *Macromolecules* 1995, 28, 1721.
4. Percec, V.; Barboiu, B. *Macromolecules* 1995, 28, 2970.
5. Granel, C.; Dubois, P.; Jermoe, R.; Teyssier, P. *Macromolecules* 1996, 29, 8576.
6. Gynor, SG.; Matyjaszewski, K. *Macromolecules* 1997, 30, 4241.
7. Jankova, K.; Chen, XY.; Kops, J.; Batsberg, W. *Macromolecules* 1998, 31, 538.
8. Jankova, K.; Kops, J.; Chen, XY.; Batsberg, W. *Macromol Rapid Commun* 1999, 20, 219.
9. Li, Z.C. ; Liang , Y.Z. ; Chen, G.Q. ; Li, F.M., *Macromol Rapid Commun* 2000, 21, 375.
10. Reining, B.; Keul, H.; Hocker, H. *Polymer* 1999, 40, 3555.
11. Bednarek, M.; Biedron, T.; Kubisa, P. *Macromol Rapid Commun* 1999, 20, 59.
12. Ibrahim, K.; Löfgren, B.; Seppälä, J. *Eur Polym J* 2003, 39, 939.
13. Ibrahim, K.; Löfgren, B.; Seppälä, J. *Eur Polym J* 2003, 39, 2005.
14. Ibrahim, K.; Yliheikkilä, K.; Abu-Surrah, A.; Löfgren, A.; Leskelä, M.; Lappalainen, K.; Repo, T.; Seppälä, J. *Eur Polym J* 2004, 40, 1095.
15. Matyjaszewski, K.; Wei, M.; Xia, J.; McDermott, N. *Macromolecules* 1997, 30, 8161.
16. Ando, T.; Kamigaito, M.; Sawamoto, M. *Macromolecules* 1997, 30, 4507.
17. Wang, X-S.; Luo, N.; Ying, S-K.; Liu, Q. *Eur Polym J* 2000, 36, 149.
18. Even, M.; Haddleton, D.; Kukulj, D. *Eur Polym J* 2003, 39, 633.

19. Krishan, R.; Sabdham, K.; Srinivasan, V. *Eur Polym J* 2003, 39, 205.
20. Moineau, G.; Minet, M.; Dubois, Ph.; Teyssie, Ph.; Senninger, T.; Jerome, R. *Macromolecules* 1999, 32, 27.
21. Qin, S-H., Qiu, K-Y.; Swift, G.; Westmoreland, D. G.; and Wu, S. *J. Pol. Sci.: Part A: Polymer Chemistry* 1999, 37, 4610
22. Fernandez-Garcia, M., de la Fuente, J. L., Cerrada, M. L., Madruga, E. L. *Polymer* 2002, 43, 3173.
23. Fernandez-Garcia, M., Cuervo-Rodrigues, R., Madruga, E. L. *J. Appl. Pol. Sci.* 2001, 82, 14.
24. Martin-Gomis, L., Fernandez- Garcia, M., de la Fuente, J. L., Madruga, E. L., Cerrada, M. L. *Macromol. Chem. Phys.* 2003, 204, 2007.
25. Boschet, F.; Branger, C.; Margaillan, A. *Eur Polym J* 2003, 39, 333.
26. Müller, A. J.; Balsamo, V.; Arnal, M. L.; Jakob, T.; Schmalz, H.; Abetz, V. *Macromolecules* 2002, 35, 3048.

Figure 1

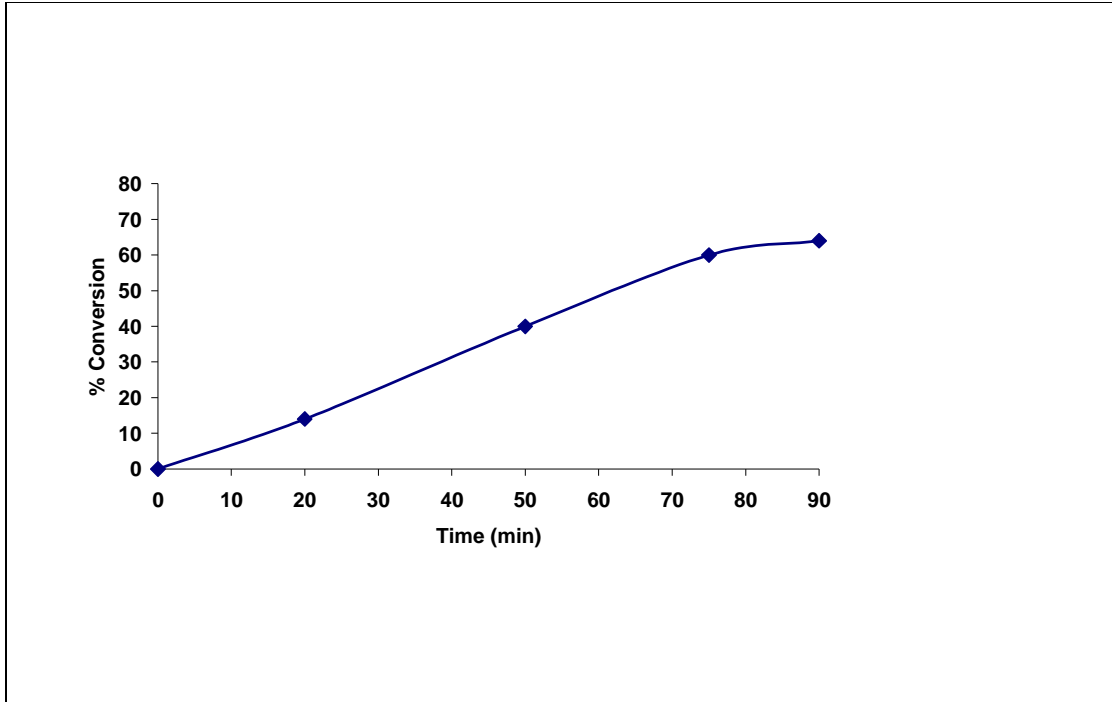


Figure 2

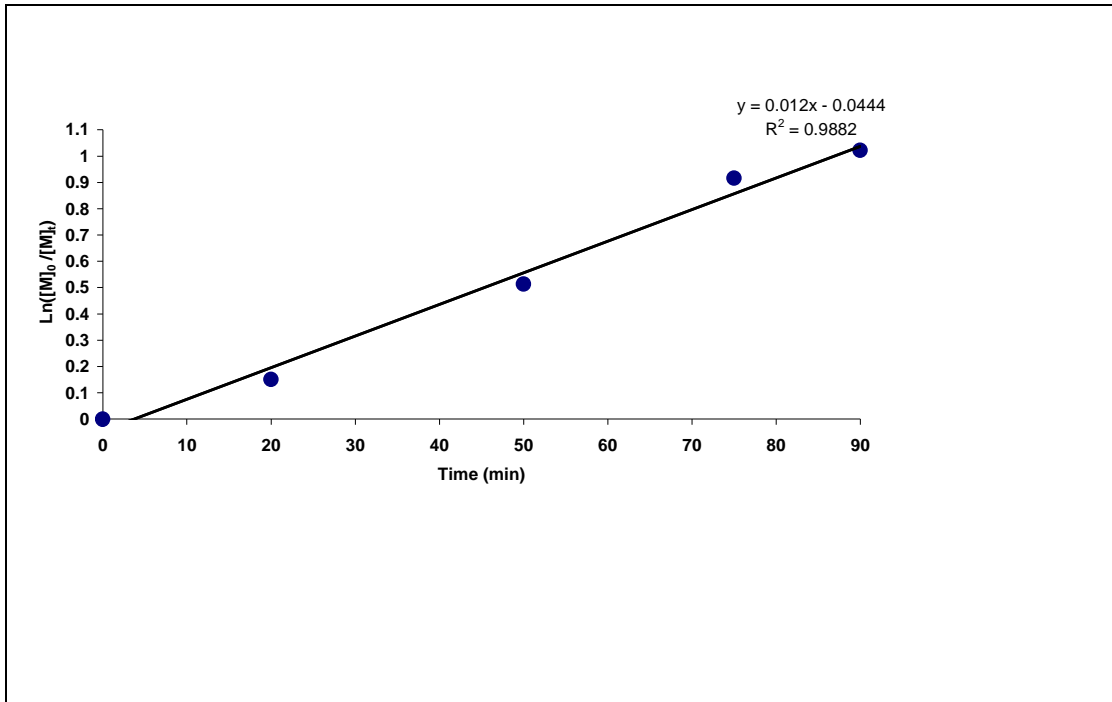


Figure 3

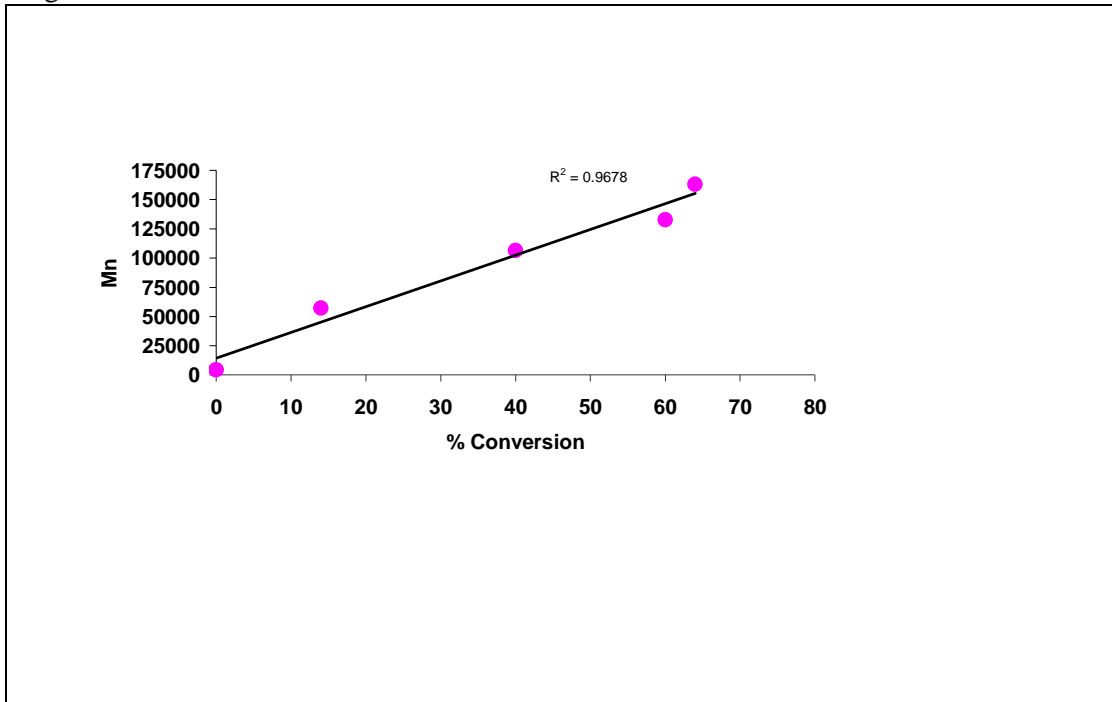


Figure 4

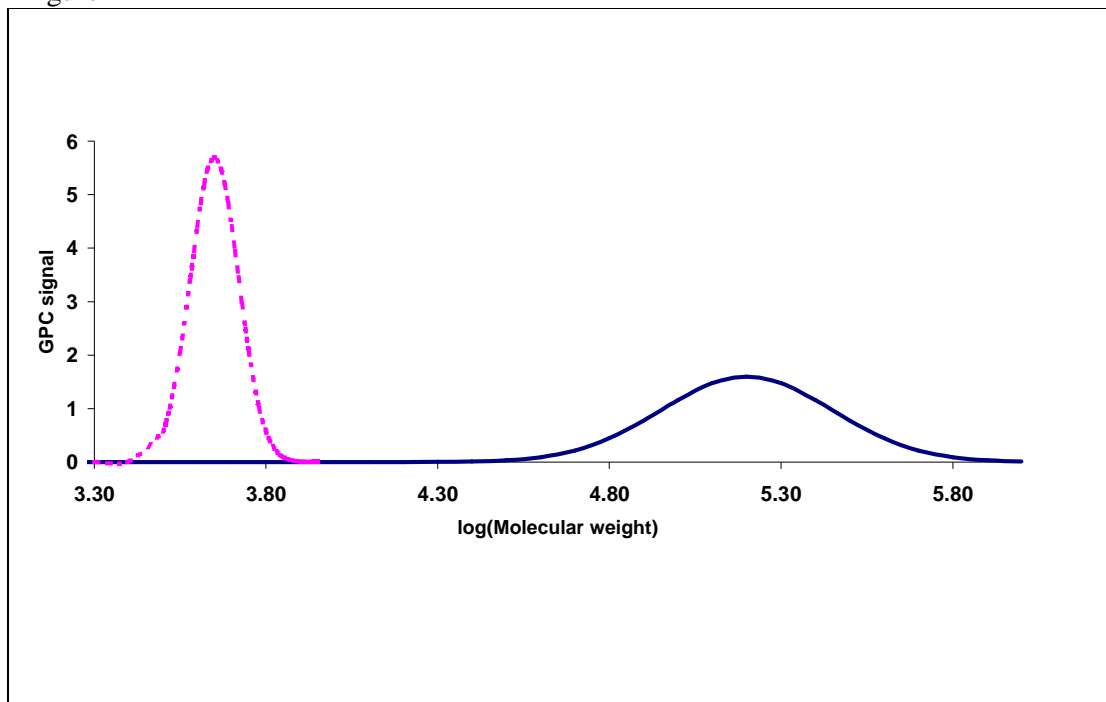


Figure 5

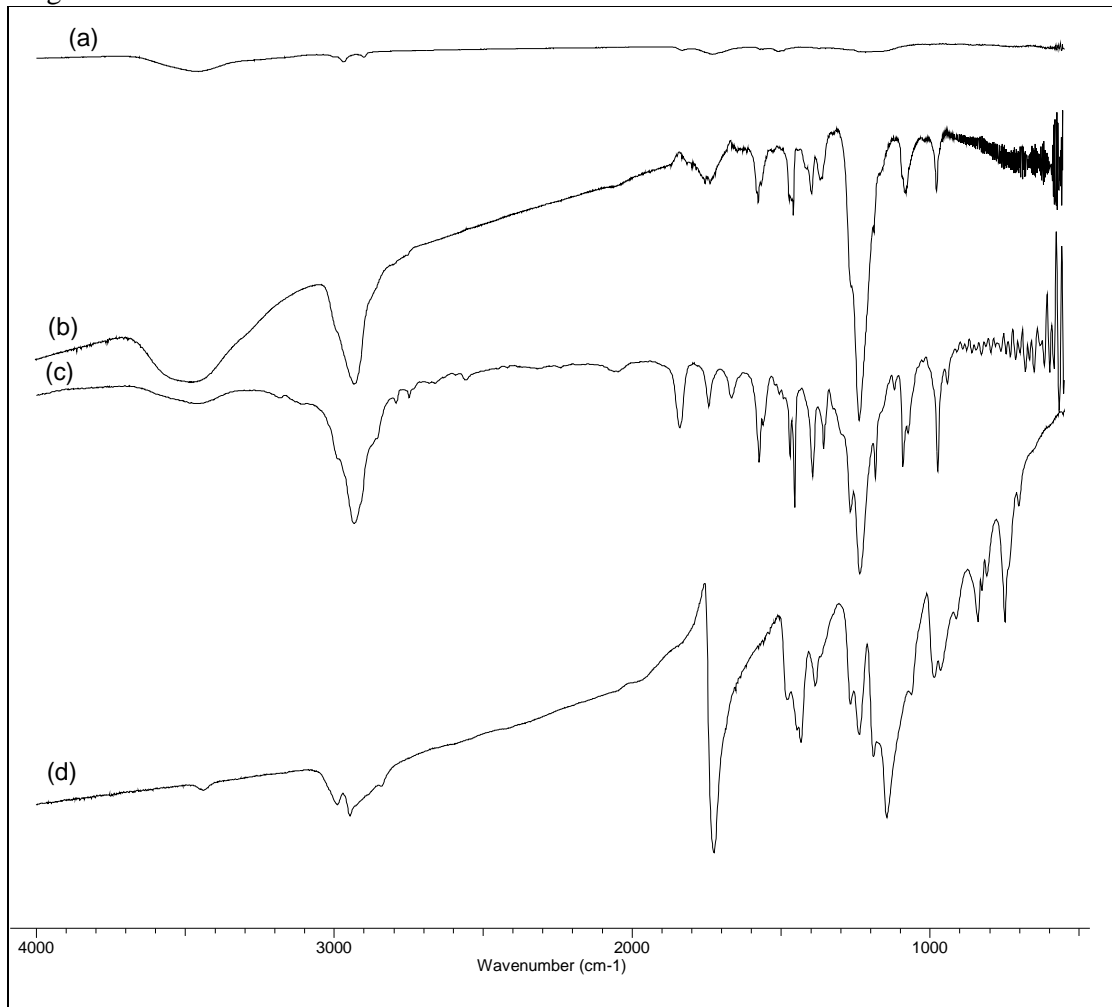


Figure 6

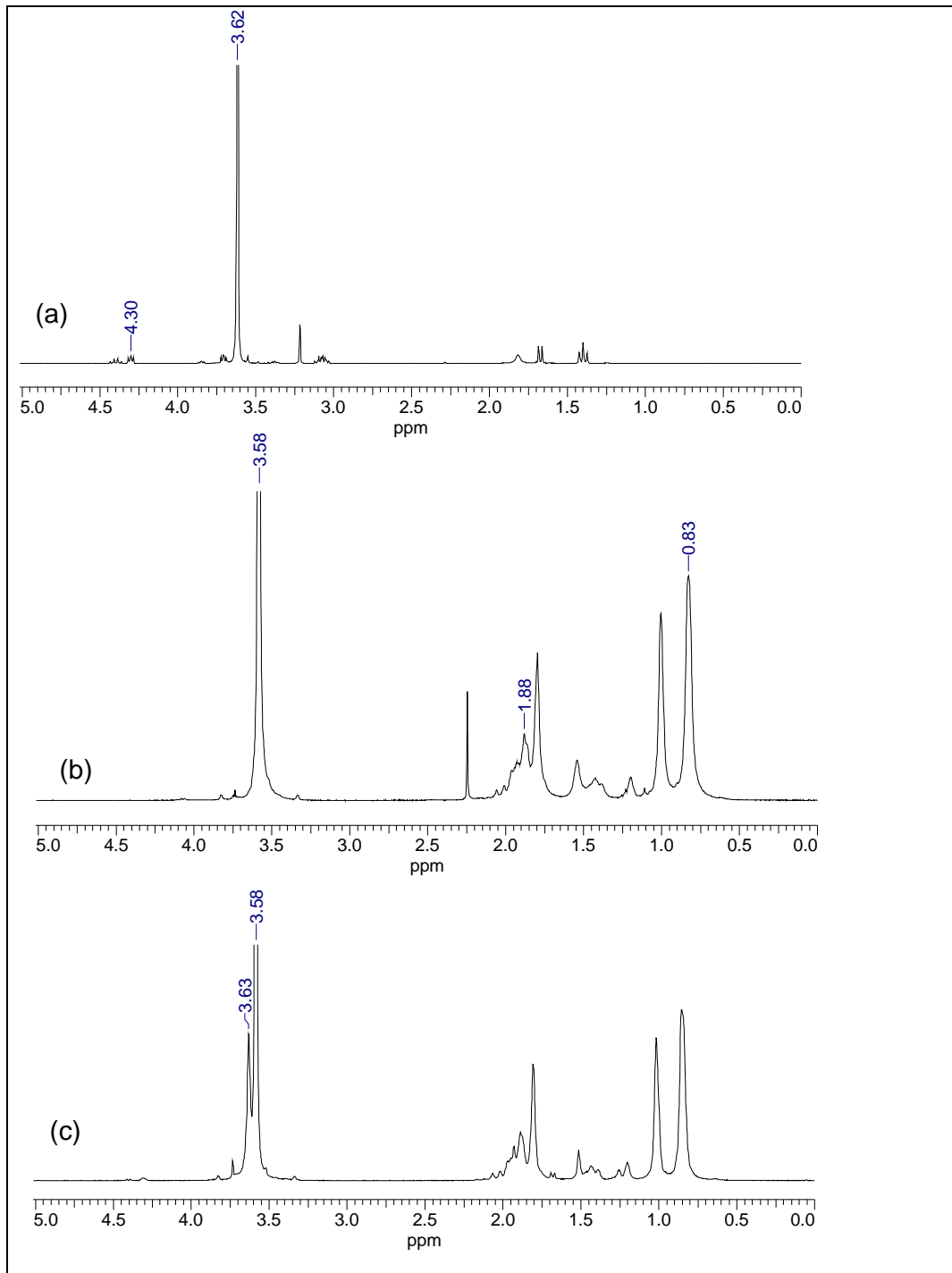


Figure 7

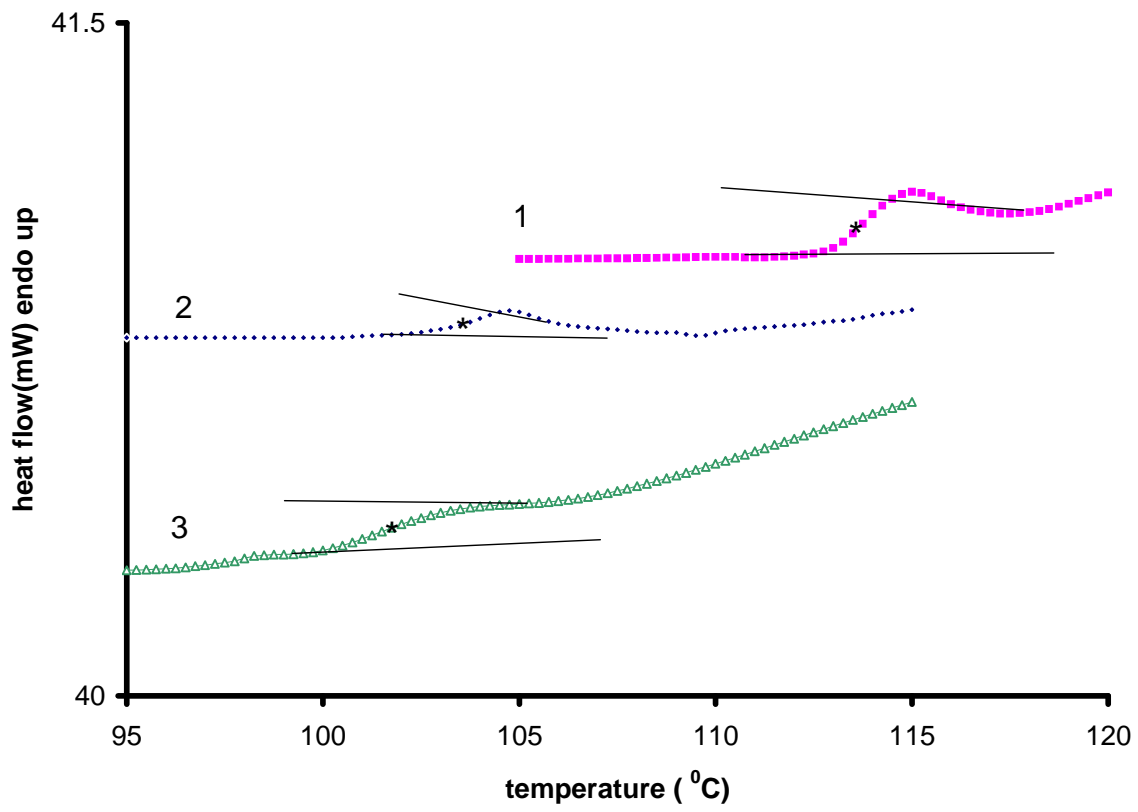


Figure 8

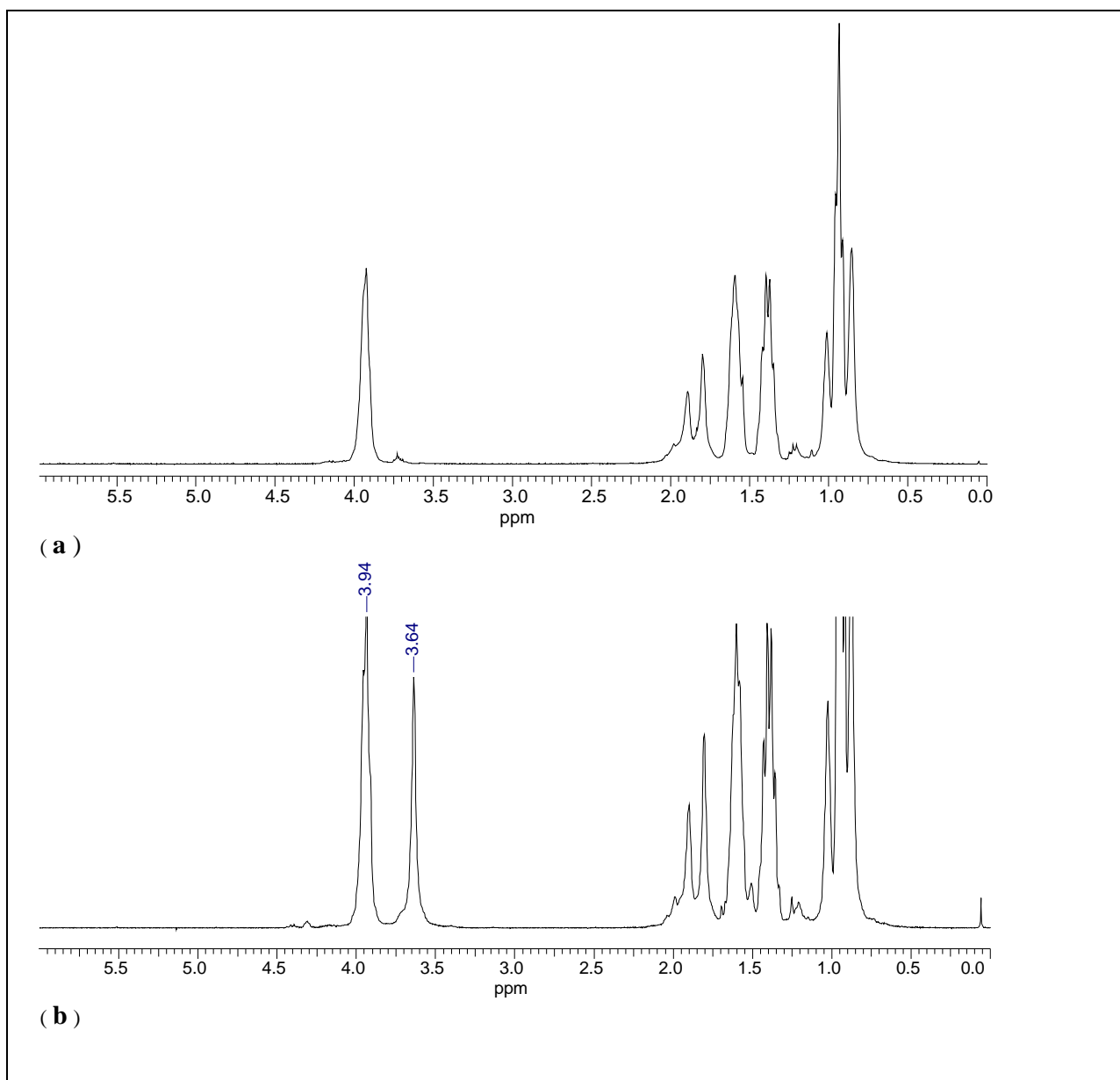


Figure 9

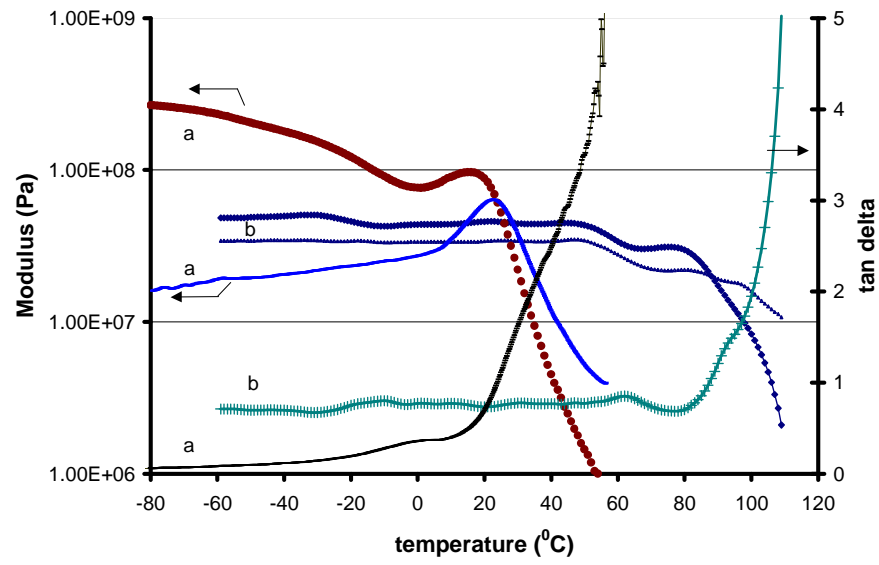


Figure 10

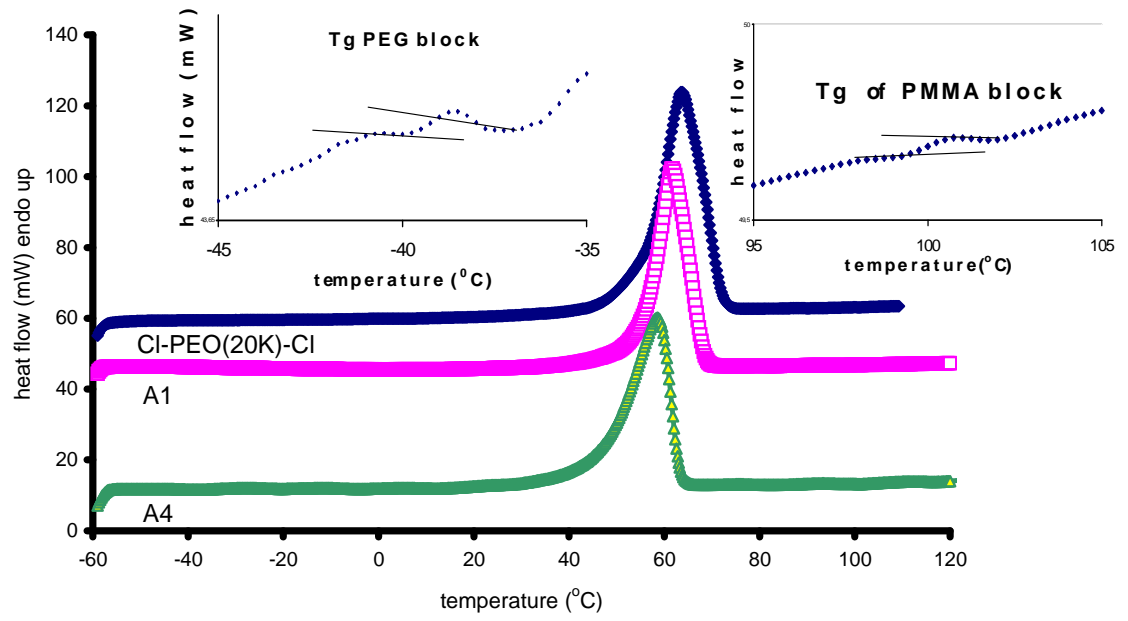


Table 1

Polymer	Mn,theo	Mn,NMR	GPC results	
			Mn	Mw/Mn
PEG 2000	2000	2050	3935	1.03
Cl-PEO-Cl	2180	2270	4300	1.03

Table 2

Sample	% conversion	Mn(GPC) ^a	Mn,theo ^b	Mw/Mn
1	14	57200	8500	1.65
2	40	105600	16300	1.58
3	60	132800	22300	1.55
4	64	163100	23500	1.47

^a Estimated by Polystyrene-calibrated SEC.

^b $Mn,theo = ([monomer]/[macroinitiator] \times Mwt \text{ of monomer} \times \text{conversion})/100 + Mwt \text{ of macroinitiator}$.

Table 3

Sample	%MMA	Mn(theo)	Mn(GPC)	Mw/Mn	Solubility in water
A1	5	21200	34700	1.21	soluble
A2	8	22000	32200	1.13	soluble
A3	15	23500	28000	1.25	dispersable
A4	20	25100	31000	1.27	dispersable
B	9	11000	15500	1.31	soluble
C1	5	6300	13200	1.02	soluble
C2	8	6500	12000	1.15	soluble
C3	15	7100	13000	1.03	dispersable
D1	5	2100	4800	1.09	soluble
D2	8	2200	5000	1.16	soluble

Table 4

Polymer	T _m (°C)	T _c (°C)	T _g PEG (°C)	T _g PMMA (°C)
PMMA				122
PEG 20K	68	37	-39	
PEG 10K	68	38	-42	
PEG 6K	65	40	-39	
PEG 2K	61	26	-40	
macroinitiator				
Cl-PEO(20K)-Cl	64	35	-39	
Cl-PEO(10K)-Cl	61	32	-39	
Cl-PEO(6K)-Cl	55	28	-39	
Cl-PEO(2K)-Cl	43	21	-37	
blockcopolymer				
A1	62	30	-39	100
A2	63	26	-39	100
A3	58	24	-39	100
A4	59	25	n.d.	100
B	56	1+(32)	-39	100
C1	56	27	-39	100
C2	54	26	-39	100
C3	51	21	-39	99
D1	43	15	-39	99
D2	44	17	-39	99

Figure Captions

Figure 1. Bulk polymerization of MMA with poly(oxyethylene) chloro telechelic as the macroinitiator and $\text{FeCl}_2 \cdot 4\text{H}_2\text{O}(\text{PPh}_3)_2$ as the catalyst at 90°C .
[Monomer]:[Macroinitiator]:[Catalyst] = 300:1:1.

Figure 2. First order kinetic plot of $\ln([M]_0/[M]_t)$ versus time in the bulk polymerization of MMA with poly(oxyethylene) chloro telechelic macroinitiator and $\text{FeCl}_2 \cdot 4\text{H}_2\text{O}(\text{PPh}_3)_2$ as the catalyst at 90°C . [Monomer]:[Macroinitiator] :[Catalyst] = 300 : 1 :1.

Figure 3. Dependence of experimental molecular weights on monomer conversions in the bulk polymerization of MMA at 90°C .
[Monomer]:[Macroinitiator] :[Catalyst] = 300 : 1 :1.

Figure 4. GPC traces of macroinitiator (dotted line) and its corresponding triblock copolymer (solid line) prepared in bulk.

Figure 5. FT-IR spectrum of (a) Pure KBr disc, (b) PEG 2000, (c) poly(oxyethylene) chloro telechelic macroinitiator, and (d) PMMA-b-PEO-b-PMMA triblock copolymer.

Figure 6. $^1\text{H-NMR}$ spectrum of (a) poly(oxyethylene) chloro telechelic macroinitiator, (b) PMMA homopolymer (in solution), and (c) PMMA-b-PEO-b-PMMA (bulk) triblock copolymer.

Figure 7. Glass transition transitions of synthesized PMMA-b-PEO-b-PMMA block copolymers. 1) sample 1, 2) sample 3, 3) sample 4

Figure 8. $^1\text{H-NMR}$ spectrum of (a) *n*-BMA homopolymer, and (b) PBMA-b-PEO-b-PBMA triblock copolymer.

Figure 9. Dynamic mechanical analysis (DMA) of a) PBMA-b-PEO-b-PBMA copolymer and b) PMMA-b-PEO-b-PMMA copolymer (polymer 3).

Figure 10. Melting curves of the water-soluble triblock copolymers A1 and A4 and the corresponding macroinitiator Cl-PEO(20K)-Cl. The inserts show the T_g transitions of the PEO and the PMMA blocks, respectively.

Table captions

Table 1. Molecular weight characterization of PEG 2000 and macroinitiator thereof.

Table 2. Variation of $M_n(\text{GPC})$, $M_n(\text{theo})$, and polydispersity with conversion in the bulk polymerization of MMA using poly(oxyethylene) chloro telechelic macroinitiator. Conditions as in Figure 1.

Table 3. Characteristics of water-soluble PMMA-b-PEO-b-PMMA triblock copolymers.

Table 4. "Thermal characteristics" of PEG- homopolymers, corresponding macroinitiators, and water-soluble PMMA-b-PEO-b-PMMA triblock copolymers .